Sympathetic Cooling of Trapped Negative Ions by Self-Cooled Electrons in a Fourier Transform Ion Cyclotron Resonance Mass Spectrometer

Guo-Zhong Li, Shenheng Guan, and Alan G. Marshall
Center for Interdisciplinary Magnetic Resonance, National High Magnetic Field Laboratory, Florida State University, Tallahassee, Florida, USA

Hot electrons confined in a Penning trap at 3 tesla self-cool to near room temperature in a few seconds by emission of cyclotron radiation. Here, we show that such cold electrons can "sympathetically" cool, in ~10 s, laser desorbed/ionized translationally hot Au^- or C_{70}^- ions confined simultaneously in the same Penning trap. Unlike "buffer gas" cooling by collisions between ions and neutral gas molecules, sympathetic cooling by electrons is mediated by the mutual long-range Coulomb interaction between electrons and ions, so that translationally hot ions can be cooled without internal excitation and fragmentation. It is proposed that electrosprayed multiply charged macromolecular ions can be cooled sympathetically, in the absence of ion-neutral collisions, by self-cooled electrons in a Penning trap. (J Am Soc Mass Spectrom 1997, 8, 793–800) © 1997 American Society for Mass Spectrometry

Reduction of ion translational and internal energy prior to detection is essential for achieving ion stability as well as high mass resolving power and sensitivity in both Penning (Fourier transform ion cyclotron resonance, or FT-ICR) and Paul (quadrupole) ion trap mass spectrometry. Translational cooling is also required to relax ions to a region near the trap center for laser-induced fluorescence of mass-selected molecular ions [1].

Seven primary methods are available for translational cooling of trapped ions and/or electrons: (a) buffer gas cooling [2–5], (b) adiabatic cooling [6–8], (c) evaporative cooling [9–12], (d) radiative cooling [13], (e) resistive cooling [13], (f) laser cooling [14, 15], and (g) sympathetic cooling [16, 17]. Although widely known in the plasma physics literature [18], several of these techniques are only now penetrating the "chemical" mass spectrometry community. Specifically, (a) collisions of ions with a "buffer" gas serve to cool atomic and molecular ions in both Penning and Paul traps. In FT-ICR MS, buffer gas cooling is essential for axializing ions by azimuthal quadrupolar excitation to convert magnetron motion to cyclotron motion, effectively "shrink wrapping" an ion cloud to a compact packet [2, 3]. (b) In FT-ICR MS, if the dc trapping potential is much higher than the ion kinetic energy, ions may be cooled by adiabatically lowering the trapping voltage to allow free expansion of the ion cloud. (c) In both Penning and Paul traps [19], ions may be cooled "evaporatively" by lowering the trapping potential stepwise and allowing the (translationally) hottest ions to escape. The remaining ions then relax to a new (lower) temperature. At ultrahigh vacuum, evaporative cooling can yield very cold ions [12]. (d) In a strong magnetic field, electrons self-cool very efficiently (~1 s damping constant at 3 tesla) by radiative emission (see below). (e) Ions undergoing periodic motion in an ion trap may be cooled by their resistive heating of the external circuit connected to the trap electrodes [13]: ions dissipate energy by inducing an electric current in the circuit. Resistive cooling is especially effective for electrons and ions of low mass-to-charge ratio, m/z, in both Penning and Paul traps. (f) Atomic ions may be cooled by irradiation from opposed laser beams that reduce the ion velocity by repeated (directional) absorption and (nondirectional) emission. (g) In "sympathetic" cooling in Penning or Paul traps, self-cooled electrons or laser-cooled atomic ions can cool polyatomic ions by mutual long-range Coulomb interactions. Advantages of ion cooling for FT-ICR MS include: enhanced mass resolving power and mass accuracy, MS/MS detection efficiency, peak height-to-noise ratio, ion remeasurement efficiency, trapping efficiency for externally ejected ions, off-axis ion injection efficiency, etc.

Sympathetic cooling was first demonstrated in a storage ring by passing a velocity-matched electron beam through an ion beam circulating in the storage

Address reprint requests to Alan G. Marshall, Center for Interdisciplinary Magnetic Resonance, National High Magnetic Field Laboratory, Florida State University, 1800 E. Paul Dirac Drive, Tallahassee, FL 32310.

* Also members of the Department of Chemistry, Florida State University.

1044-0305/97/$17.00
PII S1044-0305(97)00077-9

Received February 6, 1997
Revised March 31, 1997
Accepted March 31, 1997

Table 1. Prior examples of sympathetic cooling

Reference	Cold ions	Hot ions	Final temperature of hot ions
Larson et al. [16]	Laser cooled 10^4 Be^+	10^3 Hg^+	1.8 K
Bollinger et al. [21]	Laser cooled 10^5 Mg^+	10^3 Be^+	0.25 K
Gabrielse et al. [17]	Self-cooled electrons	Antiprotons	0.1 eV
Imajo et al. [22]	Laser cooled Be^+	Cd^+	1 K
Hall et al. [25]	Electrons	Protons	5 eV

ring to reduce the translational energy of the ion beam [20]. Wineland's group carried out the first sympathetic cooling in a Penning trap [16] and sympathetically cooled Hg^+ ions to 1.6 K by laser-cooled Be^+ ions. In another experiment, Wineland's group sympathetically cooled Be^+ ions to 0.25 K and also achieved axialization of Be^+ ions by use of laser-cooled Mg^+ ions [21]. Recently, Cd^+ ions have been cooled sympathetically below 1 K by Coulomb interactions with laser-cooled Be^+ ions confined simultaneously in the same Penning trap [22]. Gabrielse et al. have demonstrated sympathetic cooling of trapped antiprotons by Coulombic collisions with self-cooled electrons in a Penning trap [17, 23, 24]; antiprotons could thus be cooled to 0.1 eV in 10 s in a Penning trap at 6 tesla. Recently, Hall and Gabrielse [25] have cooled protons from ~60 to ~5 eV by cooling electrons in a nested Penning trap, thereby achieving the first demonstration of sympathetic cooling of ions by simultaneously trapped ions of opposite charge. Prior examples of sympathetic cooling are summarized in Table 1. In this article, the first application of sympathetic cooling for FT-ICR mass spectrometry is demonstrated.

Electron Self-cooling

Charged particles exhibit three natural motions in a Penning trap (i.e., a region of spatially homogeneous magnetic field) and axial (along the magnetic field direction) three-dimensional quadrupolar electrostatic potential [13]: cyclotron rotation at frequency, ω_+, magnetron rotation at frequency, ω_-, and axial linear oscillation at frequency, ω_z.

$$\omega_\pm = \frac{\omega_c}{2} \pm \sqrt{\frac{\omega_c^2}{4} - \frac{\omega_z^2}{2}} \tag{1}$$

$$\omega_z = \sqrt{\frac{2\alpha q V_T}{ma^2}} \tag{2}$$

in which

$$\omega_c = \frac{qB}{mc} \quad \text{(cgs units)} \tag{3}$$

is the "unperturbed" ion cyclotron frequency (i.e., cyclotron frequency in the absence of electric field), a is a trap geometric factor (2.77373 for a cubic trap) [26], q and m are ion charge and mass, V_T is the voltage applied to each end cap electrode, a is the length of one side of the cube, and c is the speed of light. For electrons at B = 3 T, a = 4.60 cm, and V_T = 9 V,

$$\frac{\omega_+}{2\pi} = 84 \text{ GHz}, \frac{\omega_-}{2\pi} = 0.72 \text{ kHz}, \tag{4}$$

$$\frac{\omega_z}{2\pi} = 11 \text{ MHz, and } \frac{\omega_c}{2\pi} = 84 \text{ GHz}$$

Radiative Damping

By Maxwell's laws, an accelerating charge radiates electromagnetic waves, thereby continuously losing (kinetic) energy [27]. It is well known that this radiation damps the charged particle's motion [28]. Because the transition probability for such electric dipole radiation is proportional to the square of the oscillation or rotation frequency of the charge, appreciable radiative decay occurs only for high-frequency motions [13]. Thus, for protons or heavier ions in FT-ICR MS, the (cyclotron) motional frequencies fall in the radiofrequency range, and radiative decay is negligibly slow (e.g., 5.9×10^7 year time constant for singly charged ions of 100 u at 3 tesla). Radiative decay is also negligible for electron magnetron motion, and is slow even for electron axial oscillation (e.g., 266-day time constant at −9 V trapping potential in a 1.875-in. cubic trap). However, electron cyclotron rotation in a strong magnetic field is so fast that radiative decay becomes the dominant energy relaxation mechanism at low neutral pressure ($\leq 10^{-8}$ torr).

Following Feynman's treatment of the theory of radiation damping [29], Comisarow [30] noted that radiation damping of molecular ions in ICR is negligible as a relaxation mechanism. However, cooling of electrons by radiative damping in ICR was not considered by Comisarow.

Brown and Gabrielse [13] evaluated the radiative damping rate constant for ions in a Penning trap:

$$\frac{dE}{dt} = -\gamma_c E \tag{5}$$

$$E(t) = E_0 \exp(-\gamma_c t) \tag{6}$$

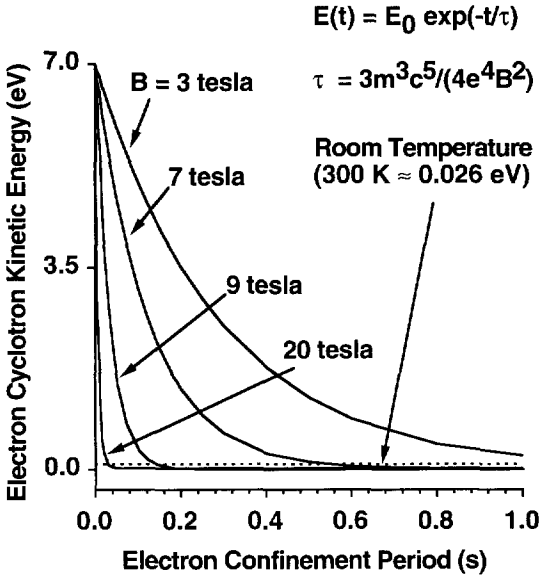

Figure 1. Electron cyclotron kinetic energy vs. time during the period of electron confinement in the analyzer trap, for each of several magnetic field strengths. Note that electrons self-cool in a few seconds at 3 tesla by radiative emission.

$$\gamma_c = \frac{4e^2\omega_+^2}{3m_ec^3}\frac{\omega_+}{\omega_+ - \omega_-} \approx \frac{4e^2\omega_c^2}{3m_ec^3} \quad \text{(cgs units)} \qquad (7)$$

in which E, r, e, and m_e are the cyclotron energy, cyclotron radius, elementary charge, and electron mass. For electrons in a 3 tesla magnetic field, the time constant, τ, for exponential decrease in electron cyclotron energy, is

$$\tau = \gamma_c^{-1} = 0.29 \text{ s} \qquad (8)$$

The experimental value of τ is a few times longer than the value calculated from eq 8, because the Penning trap electrodes do not provide an ideal microwave cavity for electron cyclotron radiation [13].

Figure 1 shows electron cyclotron (kinetic) energy as a function of time, for electrons of 7 eV initial cyclotron kinetic energy, in magnetic fields of 3, 7, 9, and 20 tesla. Note the much faster self-cooling at higher magnetic field. Moreover, because of imperfectly quadrupolar electrostatic trapping potential, electron cyclotron rotation will couple with axial oscillation [23, 31, 32]. Thus, radiative self-cooling of electron cyclotron motion will also effectively cool electron axial motion, and the electrons should quickly cool to near room temperature in a few seconds even at a magnetic field of 3 tesla.

Sympathetic Cooling

In "buffer gas" cooling, a cold neutral gas cools translationally hot ions by ion-neutral collisions. In "sympathetic" cooling, cold electrons or ions cool translationally hot ions by electron-ion or ion-ion Coulomb interactions. The exponential time constant, τ, for energy damping by sympathetic cooling is given by [33]

$$\tau(\text{cooling}) = \frac{3m_cm_Hc^3}{8(2\pi)^{1/2}n_cq_c^2q_H^2 \ln \Lambda} \cdot \left(\frac{kT_c}{m_cc^2} + \frac{kT_H}{m_Hc^2}\right)^{3/2} \quad \text{(cgs units)} \qquad (9)$$

in which m_c, q_c, T_c and m_H, q_H, T_H are mass, charge and temperature of cold and hot ions; n_c is the number density of cold ions; c is the speed of light; and k is Boltzmann's constant. ln Λ arises from a cutoff in the integration over impact parameters due to Debye shielding of the Coulomb force; ln Λ has typical values of 10–20 during the cooling process [23].

As an example, for sympathetic cooling of trapped negative Au^- ions by self-cooled electrons, $m_c = m_e$, $q_c = e$, $n_c = n_e = 10^7$ cm^{-3} [the maximum density for electrons in a 3 tesla Penning trap is n_e (max) $\approx 4 \times 10^{13}$ cm^{-3}], $kT_c = 0.026$ eV (room temperature), ln $\Lambda = 15$, $m_H = 197$ u, $q_H = e$, and $kT_H = 2$ eV we have

$$\tau(\text{cooling}) \approx 2 \text{ s} \qquad (10)$$

The cooling time for highly charged ions (as from electrospray ionization) will be even shorter because (see eq 9) τ(cooling) is inversely proportional to the square of ion charge.

The ion initial energy distribution is determined by the ion source: translationally hot molecular ions may result from matrix-assisted laser desorption (MALDI) or electrospray ionization (ESI). Thereafter, cold ions such as self-cooled electrons and laser-cooled atomic ions can reach thermal equilibrium rapidly [34–36].

Experimental

The present experiments were conducted with a 3 tesla FTMS-2000 instrument (Finnigan FTMS, Madison, WI) equipped with 1.875-in. dual cubic traps (Figure 2), and an Odyssey® data system. Laser desorption/ionization was performed with a Nd:YAG laser (Surelite I, Continuum, Santa Clara, CA) operated at 532 nm (~100 mJ/pulse) or 1064 nm (~300 mJ/pulse), with a pulse width of ~6 ns. The Nd:YAG laser beam was directed through a quartz window on the analyzer side of the main vacuum chamber and focused by a 1 m focal length lens through a 2 mm diameter conductance limit to a spot size of ~0.5 mm^2 on the probe on the source side of the main vacuum chamber. A pulse of electrons was generated by a voltage gate in front of a filament outside the magnet cryostat. Figure 3 shows the method of trapping electrons. Electrons are trapped by raising the analyzer end cap potential to admit electrons and then lowering the potential on the analyzer end cap to confine electrons for subsequent self-cooling and sympathetic cooling.

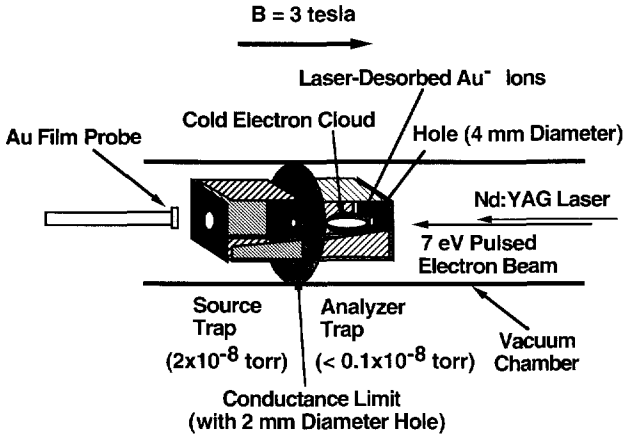

Figure 2. Schematic diagram of a dual cubic Penning trap for production of self-cooled trapped electrons for sympathetic cooling of trapped negative ions.

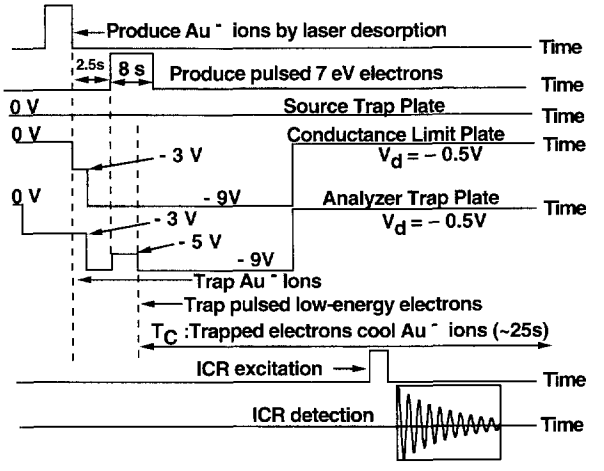

Figure 4. FT-ICR MS experimental event sequence for sympathetic cooling of trapped negative Au^- ions by self-cooled electrons (see text).

Figure 4 shows the FT-ICR MS experimental event sequence. Hot Au^- ions were generated from a thin (20 nm) gold film on glass [37] by laser desorption and allowed to enter the analyzer trap by setting the voltage on the conductance limit to 0 V. The source end cap was held at 0 V during laser desorption. The conductance limit voltage was then decreased to −3 V from 0 V to confine Au^- ions in the analyzer trap after Au^- ions were allowed to pass from the source trap through a 2 mm conductance limit plate (see Figure 2). The analyzer end cap was held at −3 V during the gated trapping of Au^- ions. After 0.5 s of trapping Au^- ions, both the conductance limit voltage and analyzer end cap voltage were decreased from −3 to −9 V. After another 2 s of waiting, the electron gun gate was opened for 8 s. Therefore, the total time elapsed between the generation of Au^- ions and the generation of electrons was 2.5 s. During this period, neutral Au atoms were pumped away (see next section). Next, the electron gate was opened and the analyzer end cap voltage was increased from −9 to −5 V for 3 s (at this potential, Au^- ions remained trapped in the analyzer trap), as shown in Figure 3. During this period some electrons from the hot-filament electron gun (~7 eV kinetic energy, ~5 μA current) may be trapped in the analyzer compartment. Immediately thereafter, the analyzer end cap voltage was decreased from −5 to −9 V to provide for gated trapping of electrons. It is estimated that ~10,000,000 electrons were captured in the trap. Once the electrons are inside the analyzer trap, the analyzer end cap voltage was held at −9 V to confine both electrons (and Au^- ions) for 20 s or more. During that time, the trapped electrons self-cool by cyclotron radiation (in a few seconds) and the cold electrons then sympathetically cool the Au^- ions. Finally, the analyzer end cap and conductance limit potentials were increased to −0.5 V, and dipolar cyclotron excitation/detection was used to see if the Au^- ions are sufficiently cold to remain trapped. (In a separate control experiment, the same steps were repeated, but without the pulse of electrons.) Coherent ICR motion was excited by dipolar frequency-sweep excitation (~80 $V_{(p-p)}$, (2.7 kHz–2.4 MHz at a sweep rate of 400 Hz/μs). Fourier transformation of the resulting time-domain signal (128 K data points) without zero-filling or apodization, followed by magnitude calculation and frequency-to-mass conversion yielded FT-ICR mass spectra shown in Figure 5. C_{70}^- was detected with similar procedures to yield the spectra shown in Figure 8, with modifications noted below (e.g., excitation from 3–475 kHz at a sweep rate of 400 Hz/μs).

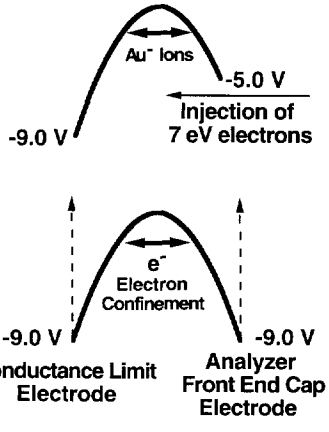

Figure 3. Electrostatic potential along the magnetic field (axial) direction in the analyzer Penning trap. Top: during electron injection. Bottom: during electron confinement period. Electrons are trapped by raising the analyzer end cap potential to admit electrons (top) and then lowering the potential on the analyzer trap plate to confine electrons for subsequent self-cooling and for sympathetic cooling of negative ions.

Results and Discussion

Au^- ions produced by Nd:YAG laser desorption have high initial kinetic energy, but may be still confined in

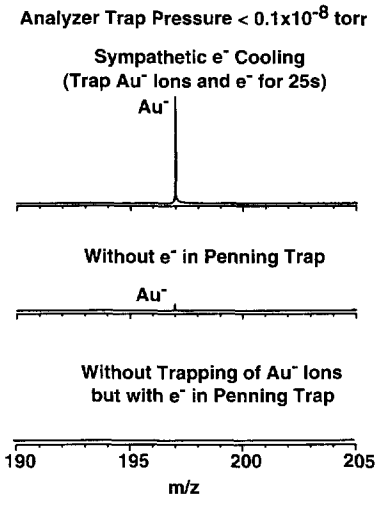

Figure 5. Negative Au^- ions with (top) and without (middle) sympathetic cooling for 25 s by trapped electrons, and (bottom) without trapping of Au^- ions, but with trapped electrons. See text for details.

a Penning trap by setting the trap voltage to −3 V (Figure 6b). However, if the trap voltage is increased from −9.0 V to the range of −0.2 to −0.8 V, most of the ions escape from the trap (Figure 5, middle spectrum and Figure 6b). In contrast, if the Au^- ions are confined in the same trap in the presence of (rapidly self-cooled) electrons, the Au^- ions are quickly cooled to near room temperature (<0.13 eV) by the cold electrons; the trap voltage may then be increased from −9.0 V to the range of −0.2 to −0.8 V while still confining the (now cold) Au^- ions, as evidenced by their strong FT-ICR mass spectral signal [Figure 5 (top) and Figure 6a]. For a trap potential of −0.2 V, the well depth of a cubic trap is (2/3) 0.2 eV ≈ 0.13 eV. Therefore, based on the strong FT-ICR signal for Au^- ions at −0.2 V trapping voltage in Figure 6a, the Au^- ion kinetic energy must be less than 0.13 eV.

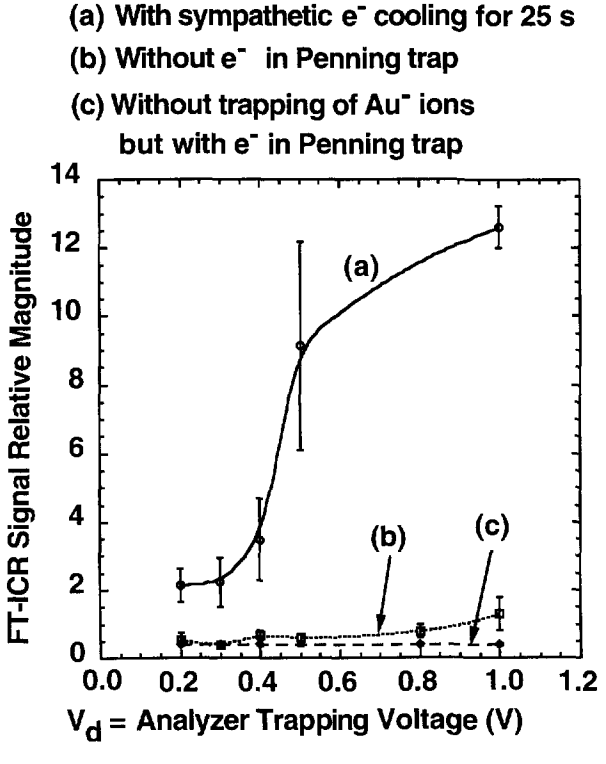

Figure 6. Negative Au^- ions, (**a**) with and (**b**) without sympathetic cooling for 25 s by trapped electrons, and (c) without trapping of Au^- ions, but with trapped electrons for different lowered analyzer trap voltages, V_d (V). Each data point represents an average of three measurements, and the error bar [too small to show in (c)] is the standard deviation.

Can Cold Penning-trapped Electrons Attach to Laser-Desorbed Neutral Au Atoms in this Experiment?

The answer is no, for three reasons. First, relatively few neutral Au atoms are generated by laser desorption in 10 ns. The laser spot diameter is ~0.5 mm^2 and the gold film is ~20 nm thick. Therefore, it can be estimated that the sum of Au atoms and Au ions as $\sim 10^{17}$ per laser pulse (for an Au atomic volume of $\sim 14 \times 10^{-3}$ nm^3). During laser desorption the ion gauge reading in the source trap side did not change. Therefore, we believe that the Au atoms are quickly pumped out by the 2000 L/s cryopump. Second, our sympathetic cooling experiment is performed in the analyzer trap, and the number of Au atoms that transit the 2 mm conductance limit to enter the analyzer trap will be even smaller. (During laser desorption/ionization the ion gauge in the analyzer trap side also did not change.) Third, the most solid evidence is the experimental result. The interval between laser desorption/ionization and generation of pulsed electrons is 2.5 s (see Figure 4). To check that all the Au atoms in the analyzer trap are pumped out during this period, we increased both the conductance limit voltage and analyzer end cap voltage to 0 from −3 V so that Au^- ions are not captured in the analyzer trap during the laser desorption/ionization step. Then, 0.5 s after laser desorption/ionization, we dropped both the conductance limit voltage and analyzer end cap voltage to −9 from 0 V. After waiting for 2.5 s after laser desorption/ionization, the electron gate was opened and electrons were trapped in the analyzer trap. After waiting another 28 s both the conductance limit voltage and analyzer end cap voltage were increased to 0.5 V and ICR excitation/detection performed. The bottom mass spectrum in Figure 5 shows no FT-ICR signal from Au^- ions when the dc trapping potential in the analyzer trap is set to zero during the laser desorption process (with all other parameters unchanged). Figure 6c also gives evidence of no Au^- ions when the dc trapping potential in the analyzer trap is set to zero during the laser desorption process for each of several analyzer trap voltages during the FT-ICR measurement. Therefore, it is believed that the Au^- ions detected in Figure 5 (top), Figure 6a, and Figure 7a (see below) cannot

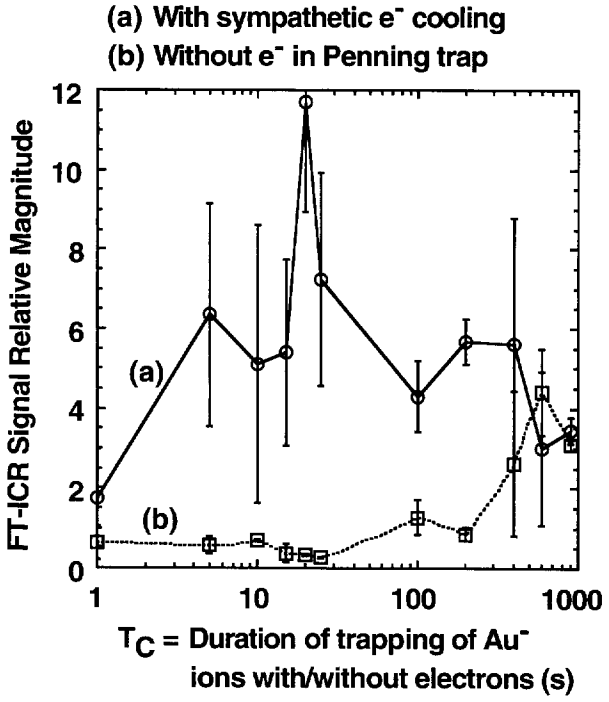

Figure 7. Negative Au^- ions (**a**) with and (**b**) without sympathetic cooling by trapped electrons at lowered analyzer trap voltage, $V_d = -0.5$ V for different periods of trapping of Au^- ions with/without electrons. Each data point represents an average of three measurements, and the error bar is the standard deviation.

result from attachment of cold electrons to neutral Au atoms produced by laser desorption. In summary, sympathetic electron cooling for 25 s (Figure 6a) obviously produces a much larger FT-ICR signal at any trapping voltage during data acquisition than without electrons in the analyzer trap (Figure 6b) or without trapped Au^- ions in the analyzer trap during the laser desorption process (Figure 6c).

Cooling by Background Buffer Gas

The pressure in the source trap is $\sim 2 \times 10^{-8}$ torr. Because our ion gauge can register pressure only down to 1×10^{-9} torr, the pressure in analyzer trap is probably at most $\sim 1 \times 10^{-9}$ (given that the ion gauge reading is 0×10^{-9} torr). The collision rate between Au^- ions with background gas is

$$\gamma_{\text{collision}} = n_B \sigma v \tag{11}$$

in which n_B is the number density of background neutral gas molecules, σ is the cross section for collisions between Au^- ions with background gas, and v is Au^- ion velocity. For the background gas at room temperature and 1×10^{-9} torr pressure, $n_B \approx 3 \times 10^7$ cm^{-3}.

For an assumed collision cross section, $\sigma \approx 10^{-15}$ cm^2, the collision rate for Au^- ions at 2 eV kinetic energy ($v \approx 1.4 \times 10^5$ cm s^{-1}) is

$$\gamma_{\text{collision}} = (3 \times 10^7 \text{ cm}^{-3}) \times (10^{-15} \text{ cm}^2) \times (1.4 \times 10^5 \text{ cm s}^{-1}) = 4.2 \times 10^{-3} \text{ s}^{-1} \tag{12}$$

Thus, the collision cooling by buffer gas can be effective only when Au^- ions are trapped for a few hundred seconds. Collisions between Au^- ions and buffer gas at less than 1×10^{-9} torr pressure cannot effectively cool Au^- ions in less than 100 s.

Figure 7 gives the experimental result of (a) sympathetic electron cooling and (b) buffer gas cooling at 1×10^{-9} torr pressure as a function of trapping period at lowered analyzer trapping voltage, $V_d = -0.5$ V (see experimental event sequence of Figure 4). From Figure 7, it is clear that the buffer gas cooling becomes effective only after a trapping interval of more than 100 s, in agreement with the calculation from eq 14. In contrast, sympathetic electron cooling becomes effective after just a few seconds of simultaneous trapping of both Au^- ions and electrons. After 500 s confinement of Au^- ions, there is no noticeable difference between sympathetic electron cooling and buffer gas cooling (without electrons). The results in Figures 5, 6, and 7 definitively establish that trapped negative Au^- ions have been sympathetically cooled by self-cooled electrons in our FT-ICR mass spectrometer.

Similar sympathetic cooling experiments with C_{70}^- ions have also been performed. C_{70}^- ions produced by Nd:YAG laser desorption have high initial kinetic energy, but may be confined in a Penning trap by applying -9 V to each end cap. However, if the trap voltage is increased from -9.0 to -0.5 V, essentially all of the ions escape from the trap (Figure 8, top mass spectrum). In contrast, if the C_{70}^- ions are confined in the same trap in the presence of (rapidly self-cooled) electrons, the C_{70}^- ions are quickly cooled to near room temperature (~ 0.025 eV) by the cold electrons; the trap voltage may then be raised from -9.0 to -0.5 V while still confining the (now cold) C_{70}^- ions, as evidenced by their strong FT-ICR mass spectral signal (Figure 8, bottom). The C_{70}^- ions detected in Figure 8 (bottom) cannot result from attachment of cold electrons to neutral C_{70}^- molecules produced by laser desorption, because no C_{70}^- is seen when the dc trap potential is set to zero during the laser desorption process (with all other parameters unchanged). Moreover, buffer gas cooling is negligibly slow at the $\sim 10^{-9}$ torr pressure in the analyzer trap. The major difference between C_{70}^- and Au^- experiments is the conductance limit diameter (5 mm for C_{70}^- ions and 2 mm for Au^- ions).

At sufficiently high electron (or ion) density, rotation of the ion clouds (both electrons and Au^- ions) about the magnetic field axis of the trap can produce a centrifugal separation of the ion species [38]. The cloud rotation frequency is like a magnetron rotation at much less than the cyclotron frequency. The rotation frequency is nearly independent of ion mass. The lighter

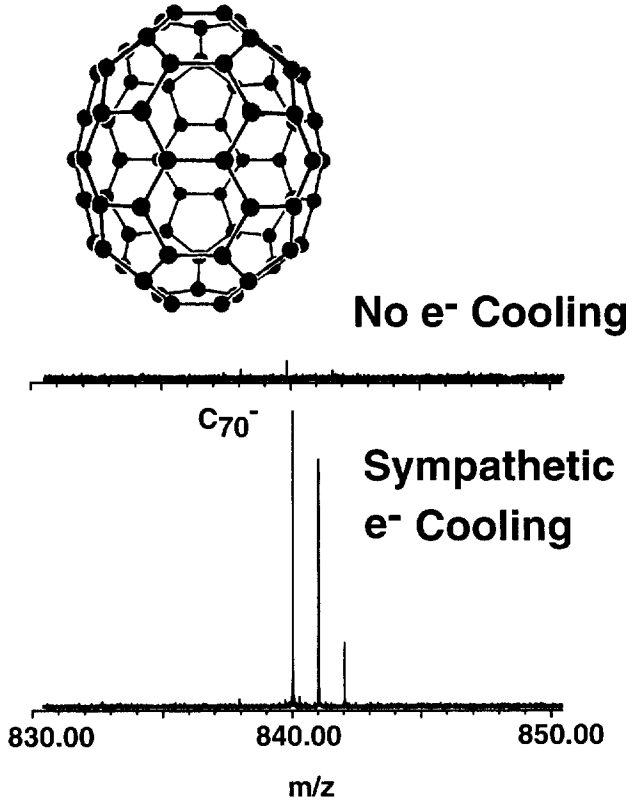

Figure 8. Negative C_{70}^- ions, without (top) and with (bottom) sympathetic cooling by trapped electrons. See text for details.

ions (electrons) tend to move radially inward (toward the trap axis), whereas the heavier ions (Au^-) move radially outward. This separation of the ions continues until both species are rotating at the same frequency. Uniform rotation is one characteristic of thermal equilibrium of a non-neutral plasma [38]. The higher-mass Au^- ions form a doughnut around the lower-mass electrons. Although the separation of the ion species limits the thermal coupling between the species, sympathetic cooling has been demonstrated in this and other experiments [16, 17, 21, 22, 25] due to the long-range nature of Coulomb interactions.

Conclusion and Future Possibilities

The present experiments suggest several other types and uses of sympathetic cooling in mass spectrometry. (a) Laser-cooled atomic positive ions could be used to cool highly charged high-mass electrosprayed molecular positive ions to ~1 K, thereby dramatically reducing both the ion cyclotron and magnetron radii. (b) Self-cooled electrons could be used to cool electrosprayed multiply charged high-mass negative ions to near chamber temperature, without fragmentation due to the long range nature of the Coulomb interaction. (c) Conceivably, self-cooled electrons could cool positive ions to near room temperature, by confining both electrons and positive highly charged electrosprayed ions simultaneously in either a nested pair of Penning traps [25, 39–41] or in a combined trap [42, 43]. In either case, the recombination rate between electrons and positive ions must be small. (d) Sympathetic cooling could be combined with two-dimensional azimuthal quadrupolar excitation [2, 3], with the "buffer gas" effectively replaced by self-cooled electrons.

Acknowledgments

This work was supported by the NSF (grant nos. CHE-93-22824 and CHE-94-13008), Florida State University, and the National High Magnetic Field Laboratory at Tallahassee, FL.

References

1. Li, G.-Z.; Vining, B. A.; Guan, S.; Marshall, A. G. *Rapid. Commun. Mass Spectrom.* **1996,** *10,* 1850–1854.
2. Savard, G.; Becker, S.; Bollen, G.; Kluge, H.-J.; Moore, R. B.; Schweikhard, L.; Stolzenberg, H.; Wiess, U. *Phys. Lett. A* **1991,** *158,* 247–252.
3. Guan, S.; Kim, H. S.; Marshall, A. G.; Wahl, M. C.; Wood, T. D.; Xiang, X. *Chem. Rev.* **1994,** *8,* 2161–2182.
4. March, R. E.; Hughes, R. J. *Quadrupole Storage Mass Spectrometry;* Wiley: New York, 1989; p 471.
5. Rempel, D. L.; Gross, M. L. *J. Am. Soc. Mass Spectrom.* **1992,** *3,* 590–594.
6. Dubin, D. H.; O'Neil, T. M. *Phys. Rev. Lett.* **1986,** *56,* 728–731.
7. Li, G. Z.; Poggiani, R.; Testera, G.; Werth, G. Z. *Phys. D* **1991,** *22,* 375–382.
8. Kastberg, A.; Phillips, W. D.; Rolston, S. L.; Spreeuw, R. J. C. *Phys. Rev. Lett.* **1995,** *74,* 1542–1545.
9. Masuhara, N.; Doyle, J. M.; Sandberg, J. C.; Kleppner, D.; Greytak, T. J.; Hess, H. F.; Kochanski, G. P. *Phys. Rev. Lett.* **1988,** *61,* 935–938.
10. Li, G. Z.; Poggiani, R.; Testera, G. *Commun. Theor. Phys.* **1993,** *19,* 1–12.
11. Adams, C. S.; Lee, H. J.; Davidson, N.; Kasevich, M.; Chu, S. *Phys. Rev. Lett.* **1995,** *74,* 3577–3580.
12. Anderson, M. H.; Ensher, J. R.; Matthews, M. R.; Wieman, C. E.; Cornell, E. A. *Science* **1995,** *269,* 198–201.
13. Brown, L. S.; Gabrielse, G. *Rev. Mod. Phys.* **1986,** *58,* 233–311.
14. Wineland, D. J. *Science* **1984,** *226,* 395–400.
15. Wineland, D. J.; Itano, W. M. *Phys. Today* **1987,** 2–8.
16. Larson, D. J.; Bergquist, J. C.; Bollinger, J. J.; Itano, W. M.; Wineland, D. J. *Phys. Rev. Lett.* **1986,** *57,* 70–73.
17. Gabrielse, G.; Fei, X.; Orozco, L. A.; Tjoelker, R. L.; Haas, J.; Kalinowsky, H.; Trainor, T. A.; Kells, W. *Phys. Rev. Lett.* **1989,** *63,* 1360–1363.
18. Itano, W. M.; Bergquist, J. C.; Bollinger, J. J.; Wineland, D. J. *Phys. Scripta* **1995,** *T59,* 106–120.
19. Schaaf, H.; Schmeling, U.; Werth, G. *Appl. Phys.* **1981,** *25,* 249–251.
20. Wolf, A.; *Hyperfine Interactions* **1988,** *44,* 217.
21. Bollinger, J. J.; Heinzen, D. J.; Itano, W. M.; Gilbert, S. L.; Wineland, D. J. *Phys. Rev. Lett.* **1989,** *63,* 1031–1034.
22. Imajo, H.; Hayasaka, K.; Tanaka, U.; Watanabe, M.; Urabe, S. *Phys. Rev.* **1996,** *A53,* 122–125.
23. Rolson, S. L.; Gabrielse, G. *Hyperfine Interactions* **1988,** *44,* 233–239.
24. Gabrielse, G.; Fei, X.; Orozco, L. A.; Tjoelker, R. L.; Haas, J.; Kalinowsky, H.; Trainor, T. A.; Kells, W. *Phys. Rev. Lett.* **1990,** *65,* 1317–1320.
25. Hall, D. S.; Gabrielse, G. *Phys. Rev. Lett.* **1996,** *77,* 1962–1965.

26. Guan, S.; Marshall, A. G. *Int. J. Mass Spectrom. Ion Proc.* **1995,** *146/147,* 261–296.
27. Jackson, J. D. *Classical Electrodynamics;* Wiley: New York, 1975; p 848.
28. Landau, L. D.; Lifschitz, E. M. *The Classical Theory of Fields;* 3rd revised English ed.; Pergamon and Addison-Wesley: Oxford and Reading, MA, 1971.
29. Feynman, R.; Leighton, R. B.; Sands, M. L. *The Feynman Lectures on Physics;* Addison-Wesley: Reading, MA, 1963.
30. Comisarow, M. B. In *Ion Cyclotron Resonance Spectrometry II;* Hartmann, H.; Wanczek, K.-P, Eds.; Springer-Verlag: Berlin, 1982; pp 484–513.
31. Mitchell, D.; Delong, S.; Cherniak, D.; Harrison, M. *Int. J. Mass Spectrom. Ion Proc.* **1989,** *91,* 273–282.
32. Mordehai, A. V.; Henion, J. D. *Rapid. Commun. Mass Spectrom.* **1992,** *6,* 345–348.
33. Spizer, L. *Physics of Fully Ionized Gases;* Interscience: New York, 1962.
34. O'Neil, T. M. In *Non-Neutral Plasma Physics;* Roberson, C. W.; Driscoll, C. F., Eds.; American Institute of Physics: New York, 1988; pp 1–27.
35. Malmberg, J. H.; Driscoll, C. F.; Beck, B.; Eggleston, D. L.; Fajans, J.; Fine, K.; Huang, X.-P.; Hyatt, W. In *Non-Neutral Plasma Physics;* Roberson, C. W.; Driscoll, C. F., Eds.; American Institute of Physics: New York, 1988; pp 28–71.
36. Brewer, L. R.; Prestage, J. D.; Bollinger, J. J.; Itano, W. M.; Larson, D. J.; Wineland, D. J. *Phys. Rev. A* **1988,** *38,* 859–873.
37. Kim, H. S.; Wood, T. D.; Lee, J.-W.; Marshall, A. G. *Chem. Phys. Lett.* **1994,** *224,* 589–594.
38. O'Neil, T. M. *Phys. Fluids* **1981,** *24,* 1447–1451.
39. Gabrielse, G.; Rolston, S. L.; Haarsma, L.; Kells, W. *Phys. Lett. A* **1988,** 38–42.
40. Vartanian, V. H.; Laude, D. A. *Org. Mass Spectrom.* **1994,** *29,* 692–694.
41. Wang, Y.; Wanczek, K.-P. *Rev. Sci. Instrum.* **1993,** *64,* 883–889.
42. Li, G.-Z.; Werth, G. *Phys. Scripta* **1992,** *46,* 587–592.
43. Gorshkov, M. V.; Guan, S.; Marshall, A. G. *Rapid Commun. Mass Spectrom.* **1992,** *6,* 166–172.